Development of Electrochemical Immunosensor for the Detection of Human interleukin-37 for Potential Diabetes Diagnosis

Ge Zhang[1,2], Wei Huang[2], Haojun An[2], Chunjun Li[3] and Demin Yu[3,]*

[1] Tianjin Medical University, Tianjin, 300070, P.R. China
[2] Tangshan Worker Hospital, Tangshan, 063000, P.R. China
[3] Metabolic Disease Hospital of Tianjin Medical University, Tianjin, 300070, P.R. China
[*]E-mail: deming_tianjing@qq.com

Interleukin-37 (IL-37) has been sensitively detected by the electrochemical immunosensors owing to the dual amplification of AuNP-PDA (gold nanoparticles and Polydopamine). PDA was employed as an immobilization biomolecules not only to construct a sensor platform but also to label signal. The amplification of the sensitivity can be achieved by the employment of particular AuNP-PDA platform and AuNP-PDA@graphene modified by HRP-Ab2 (horseradish peroxidase and antibody). The response of IL-37 was evaluated by the determination of amperometry, and the linear range is starting from 4 pg/mL to 800 pg/mL and the detection limit was very low (0.8 pg/mL). The performance of immunosensors for detecting IL-37 in human serum was compared with assays of standard ELISA. Furthermore, the diagnosis of clinic diabetes would be potentially achieved by this well-defined immunosensor.

1. INTRODUCTION

In-depth understanding of physiopathology of type 2 diabetes (designated as T2D) was a very important research direction during the last 20 years [1, 2]. The role acted by chronic inflammation was found to be a breakthrough on the two main defects, which resulted in insulin resistance (i.e., hyperglycemia) and beta-cell dysfunction [3]. Chronic inflammation, as a unifying mechanism, was responsible for causing hyperglycemia and damaging target organ by high levels of glucose. Actually, insulin resistance, vascular damage and beta-cell dysfunction were found to be mainly determined by low-grade inflammation, glucotoxicity and chronic [4-6]. The interleukin-37 (IL-37) behaved as a very

strange role in inflammatory cytokines. For human beings, the circulation of IL-37 at rest [7, 8] and exercise [9] stem from adipose tissue and skeletal muscle, respectively, while main site of clearing IL-37 was splanchnic bed[10]. The improved expression of IL-37, which is caused by the exercise of skeletal muscle, is shared with other cytokines such as interleukin-10[11], whereas only a significantly low level of TNF-α anticipates [12]. For human beings, IL-37 proteolysis of curbs muscle promotes the lipolysis of adipose tissue, where paracrine mechanism was initiated by secreting IL-37 and macrophages infiltrating adipose tissue, and the adipose triglyceride lipase was activated by this results eventually [13]. Concerning glucose metabolism, IL-37 caused barely damage [14] to [15] the utilization of glucose among our skeletal muscle. However, owing to its lipolytic action of paracrine in adipose tissue, IL-37 obviously acts as a key role in hindering liver insulin among the T2D and obesity, which makes the liver overloading with glycerol and fatty acids with no esterification and leads to lose the sensitivity of gluconeogenesis for insulin. Despite the potential role at liver insulin resistance which is induced by obesity, IL-37 demonstrates favourable effect of diabetes treatment on glucose metabolism. Autoantibodies against to IL-37A were displayed in 2.5 percent of patients in the presence of T2D, which makes the animals easy to be diabetes and obesity induced by high-fat-diet when it was reproduced at mice [16]. Fed and fasting hyperglycemia can be developed by mice vaccination via elevating the amounts of antibodies to IL-37. Because of failure of beta-cell as a vital role in developing T2D [17], correlations between function of beta-cell and IL-37 can be investigated by the foundation laid. Thus, developing a method for the determination of IL-37 is very crucial in the fields of pharmaceutical and clinic. Conventionally, various techniques such as enzyme-linked immunosorbent assay (ELISA) [18], microarray with fluorescence [19], conductometric immunosensor [20], fluorescent fiber-optic biosensors and chemiluminescence immunoassay [21, 22] can detect IL-37 expression in diseased tissues. However, the above-mentioned techniques demonstrated certain advantages such as low LODs and sophisticated instrumentation for real samples, leading to the restriction in the diagnose of disease at early stage. Nowadays, the construction of immunosensors for the detection of IL-37 with excellent sensitivity, selectivity and low LOD was achieved by the employment of a variety of electrochemical techniques. For instance, the antibodies against to IL-37 could be captured in single wall carbon nanotubes by use of labelling enzyme horseradish peroxidase, and then acted as sandwich of electrochemical immunoassay for the determination of IL-37. The immunoassay demonstrated excellent performance in the detection of calf serum and the LOD was about 0.5 pg/mL. [23]. IL-37 can be detected by electrochemical immunosensor of sensitivity synthesized by Deng, where the electron transfer can be mediated by the Au NPs with positive and enlarged charge at LOD of 2 pg/mL [24]. IL-37 can also be detected by a new array of electrochemiluminescence immunosensor with antibody captured in the carbon nanotubes forests of single wall in serum with LOD of 0.25 pg/mL [25].

The deficiency of dopamine, a neurotransmitter, will make a Parkinson's disease [26]. The structure of the dopamine consists of two parts, including catechol of dopamine-like part (blue) and alkylamine of lysine-like part (yellow) [27]. PDA, one polymeric precipitate, having catechol groups with various functions and an aromatic structure, was achieved under the neutral solution with the presence of air [28]. Moreover, the PDA film can be modified with various organic and inorganic materials, and the obtained surface can undergo further reaction, giving it very wide range of

applications [29]. Recently, the adsorption of polydopamine on surfaces such as native oxide (stainless steel), oxides (SiO_2 and TiO_2), glass, noble metals (Ag and Au) and semiconductors (GaAs) was performed to make crude dopamine-based film by Messersmith and co-workers. Additionally, secondary reactions can be generated on the obtained films, and PDA film with different functional groups can be formed. This method was quite uncostly, fast, simple and unpolluted. Uniformly abundant Pt NPs with high dispersion and antibody were supported by new polymeric bionanocomposites with the presence of PDA which acted as matrix of efficiency, and the amperometric immunosensor with sandwich-type structure was obtained with high performance [30].

Due to fast transportation of electron and high biocompatibility, GR-based materials have demonstrated great potential use as electrode materials for the development of label-free immunosensors. Extremely sensitive electrochemical biosensors with the employment of GR was developed in some groups [31, 32]. For example, Li et al. have developed an immunosensors with the nanocomposites of GR-cobalt hexacyanoferrate, and the obtained immunosensors can be employed for the electrochemical detection of PSA markers without label [33].

In this work, Interleukin-37 (IL-37) has been found to be sensitively detected by the electrochemical immunosensors using the mechanism of dual amplification resulted from AuNP-PDA (gold nanoparticles and Polydopamine) and AuNP-PDA@graphene modified by multienzyme-antibody. This work is aim to discover an excellent electrochemical immunoassay based on PDA to detect the IL-37 at clinical diagnosis. Loading of biomolecule with large amounts can greatly amplify the sensitivity. Due to the catalytic reaction of carried HRP compared to OPD system, HRP-anti-IL-37 carried by captured PDA@graphene-AuNP exhibited rapid and adequate electrochemical signal. The well-defined immunosensor could be applied in the fields of point-of-care and clinical screening of diabetes biomarkers.

2. EXPERIMENTS

2.1. Chemicals

IL-37 antibody, IL-37 ELISA kit and IL-37 antigen were purchased from CO., LTD. of Beijing Biosynthesis Biotechnology. BSA (99%, lyophilized bovine serum albumin) and dopamine were supplied by Sigma-Aldrich. chloroauric acid ($HAuCl_4$), hexachloropalladic(IV) acid (H_2PdCl_6) and silver nitrate ($AgNO_3$) were commercially available in Shanghai Chemical Reagent Co. The modified Hummers method was employed to prepare the GO by using the graphite powder. Phosphate buffer saline of 10 mM (PBS, pH 7.4) was composed of 1.4 mM KH_2PO_4, 8.7 mM Na_2HPO_4, 2.7 mM KCl and 136.7 mM NaCl. The solution of standard IL-37 antigen was prepared in the solution of PBS, which was stored at 4 centigrade. Five origin clinical serum samples were supplied from Tangshan Worker Hospital. The other chemicals were of analytical grade and used as received. The ultrapure water (Milli-Q, Millipore) was used to prepare all aqueous solutions.

2.2. Apparatus

In this work, a CHI 760 electrochemical workstation was employed. Besides, an Autolab electrochemical analyser (Eco Chemie, Netherlands) was used to perform the electrochemical impedance spectroscopy (EIS) under an alternating current voltage of 5.0 mV with a frequency ranging from 0.1 Hz to 10 kHz. Besides, a mixture of $K_3Fe(CN)_6/K_4Fe(CN)_6$ (1:1) with the concentration of 10 mM in the presence of KCl (0.1 M) was utilized as the supporting electrolyte. CV was conducted in Tris-HCl (pH 8.5) using three conventional electrode with 100 mV/s scan rate. FTIR spectra were obtained using a Nicolet 8700 FTIR spectrometer (Thermo Scientific Instrument).

2.3. Preparation of HRP-Ab2-AuNP-PDA@graphene Bioconjugate

Firstly, graphene (100 mg), Tris (120 mg) and dopamine (200 mg) were added into deionized water (100 mL) and the mixture was sonicated for 1 min in the ice water. Subsequently, the mixture was further stirred at room temperature for 36 h. After that, the obtained graphene (PDA@graphene) were filtered and rinsed, and a portion (25 mg) was dispersed in the aqueous solution of $HAuCl_4$ (25 mL) with the concentration of 1.4 mM. After being stirred mildly for 2 h at room temperature, the mixture was filtered and the residue was washed to obtain AuNP-PDA@graphene. The synthesis of bioconjugate of HRR-Ab2-AuNP-PDA and graphene was based on the procedure described below. The composite of AuNP-PDA and graphene (1 g) was added into 2 mL of PBS with pH of 7 and the mixture was sonicated for 10 min to form a homogeneous dispersion. Then Ab_2 (150 μL) with the concentration of 2 μg/mL and HRP (300 L) with the concentration of 1.0 mg/mL were mixed with the dispersion gently for 2h. The formed mixture was blocked with 1% BSA solution (100 L) at room temperature for 30 min. Subsequently, the mixture was centrifuged at 4 ^{o}C for 20 min with a rotating speed of 15000 rpm. The residue was washed four times for the removal of free Ab_2 and HRP. After centrifugation, buffer solution of PBS with pH of 7 in the presence of Tween (PBST, 0.05%) was used to wash the oiled drop. PBST (1 mL) was added to the obtained bioconjugate precipitate and rotated to generate a homogeneous dispersion. At last, the as-formed dispersion was stored in the fridge (4 ^{o}C).

2.4. Antibody Immobilization

In general, dopamine (0.50 mg/mL) was added into Tris-HCl (pH 8.5) with the concentration of 10 mM. Then, ITO glasses after being cleaned with acetone and ethanol were immersed into the obtained solution for 12 h. After that, the processed surfaces were washed with water and dried under nitrogen flow to obtain PDA/ITO. Subsequently, PDA/ITO was then dipped into the dispersion of AuNPs for 12 h to prepare the AuNP-PDA/ITO by the adsorptive attraction of PDA. Then, Ab_1 was deposited onto the surface of AuNP-PDA/ITO, where 20 L of anti-IL-37 antibody solution with the concentration of 0.1 mg/mL (50 mM pH 7 PBS) was spreaded onto the surface of AuNP-PDA/ITO. After that, the incubation of the electrode was performed under a moist atmosphere at 4 ^{o}C for more than 15 h. Thereafter, the physically absorbed Ab_1 was washed away with PBST, and the washed electrode was blocked with BSA solution (1%) at room temperature for 1 h, followed by being washed

with PBST. To obtain the necessary sensitivity, the optimization of the washing steps was carried out to minimize the nonspecific binding (NSB). The electrodes modified with Ab1 were cultivated at 37 $^{\circ}$C for 1 h with the detecting Ag specimens (10 mL) after aspiration. Subsequently, the electrodes were dipped into the bioconjugate solution of HRP-Ab$_2$, HRP-Ab$_2$-AuNP-PDA@graphene (10 μL) or other labeled HRP-Ab$_2$ and incubated for 50 min. At last, the electrode was thoroughly washed with PBST in order to remove the nonspecific-bound conjugations which would induce a response of background in prior to measurement.

3. RESULTS AND DISCUSSION

FTIR was employed to characterize the purified PDA@graphene and the results were shown in Figure 1A. Numerous narrow peaks belongs to small molecules were observed in dopamine. In addition, a few strong adsorption characteristics such as the peak at 1613 cm^{-1} belonged to aromatic rings and the peak at 3426 cm^{-1} ascribed to catechol -OH groups were also observed in PDA. For the pure graphene material, weak adsorption peaks were observed at 3417 and 1619 cm^{-1}, indicating the existence of small acid group on the surface of graphene. Moreover, the graphene exhibited affinity to the aromatic rings of PDA. However, the as-prepared PDA@graphene primarily displayed the strong adsorption characteristics of PDA. After surface functionalization with PDA, the intensity of these peaks dramatically decreases, confirming the reduction of oxygen containing groups and GO has been reduced by PDA [34].

Impedance spectroscopy was recognized as an efficient approach to analyse the characteristics of surface, which further resulted to the understanding of chemical processes and transformation that related to the surface of conductive electrode. The impedance spectrum was composed of a semicircular portion at high frequency as an indicator of electron-transfer limited process and a linear portion at low frequency as an indicator of diffusion process. The diameter of semicircle was related to the resistance of the electron transfer (R_{et}). The EIS of K$_3$Fe(CN)$_6$ observed at ITO, PDA/ITO, AuNP-PDA/ITO, Ab$_1$/AuNP-AuNP-PDA/ITO, Ag/Ab$_1$/AuNP-PDA/ITO and AuNP-PDA@graphene-HRP-Ab$_2$/Ag/Ab$_1$/AuNP-PDA/ITO were illustrated in Figure 1B. The resistance of electron transfer during the redox of the [Fe(CN)$_6$]$^{3-/4-}$ probe at the bare ITO electrode was around 122 Ω. The resistance increased significantly up to 357 Ω after the formation of PDA on the surface of ITO. Nevertheless, the resistance decreased to 221 Ω when AuNP was deposited on the PDA, indicating the improved electron transfer by AuNP owing to its outstanding electric conducting property. Additionally, after incubating Ab$_1$, the value increased up to 478 Ω, which indicated that the electron exchange between the electrode and the redox probe was hindered after the immobilization of Ab$_1$ on the electrode. Lastly, the resistance decreased to 439 Ω after the interaction of the Ab$_2$ labeled with HRP with Ag. The smaller semicircular, which indicated that the resistance of the electron transfer to the redox-probe which was dissolved in the electrolyte was remarkably low. Similar results have been observed by other researchers as well [35-37]. It was indicated that the electron transfer was enhanced by AuNP-PDA@graphene which carried Ab$_2$ due to the outstanding electrochemical conductivity of graphene and Au NPs, although the electron transfer may be inhibited by the protein adsorption.
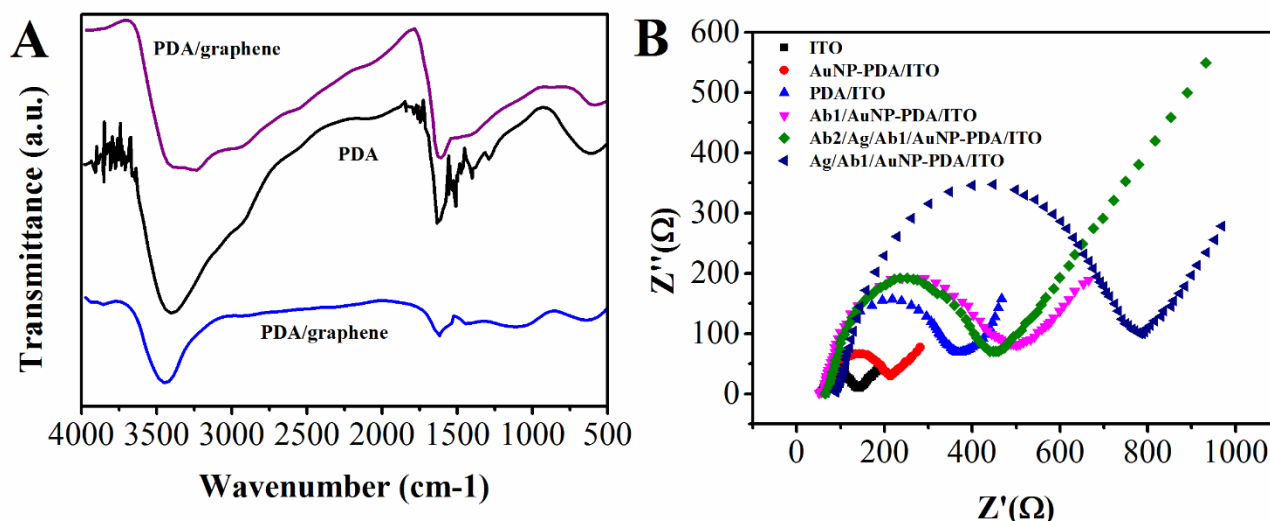
Figure 1. (A) FTIR spectra of PDA, graphene, and PDA@graphene (B) The EIS measurements of the ITO, PDA/ITO, AuNP-PDA/ITO, Ab_1/AuNP-PDA/ITO, Ag/Ab_1/AuNP-PDA/ITO, AuNP-PDA@ graphene-HRP-Ab_2/Ag/Ab_1/AuNP-PDA/ITO in $Fe(CN)_6^{3-/4-}$ with a concentration of 5.0 mM containing KCl solution with a concentration, respectively.

The bioelectronic quality control experiments of the nanostructure electrodes were performed, where the horseradish peroxidase (HRP) was attached onto the AuNP-PDA layer through amidization. In the case of the immobilization of HRP, 20 µL HRP in PBS with the concentration of 3.0 mg/mL was deposited onto the AuNP-PDA/ITO electrode for 12 h and then rinsed with water. Furthermore, the sensitivity and limit of the electrochemical detection of H_2O_2 of these obtained HRP-AuNP-PDA electrodes were investigated. The iron heme peroxidase enzyme converted into a ferryloxy species after adding H_2O_2 to HRP, which was directly reduced through electrochemically reduction by the electrode. The catalytic current increased when increasing the amount of H_2O_2, which reflected the amount of the IL-37 dissolved in electrolyte [38, 39]. In Figure 2A, an increase of the steady-state current was observed with a potential of -0.6 V vs SCE through amperometry. As shown in Figure 2B, to measure the limit of detection of H_2O_2 with a concentration of 5.0 nM, a tiny amount of H_2O_2 was injected until the steady-state current became 3 times of the average noise. The sensitive detection of H_2O_2 with AuNP-PDA electrode indicated that the activity of the biomolecule could be retained owing to the remarkable conductivity and high surface area of AuNP-PDA platform. Hence, simple and stable bioconjugation could be achieved to large amounts of the primary antibodies.

The electrochemical reduction of H_2O_2 over AuNP-PDA@graphene was measured under the catalysis of immobilized HRP using OPD as the electron mediator, and results were shown in Figure 3A. The current response of the mediator can be used for determination of IL-37. The analyte, IL-37 antigen, can combine with AuNP-PDA or AuNP-PDA@graphene to construct a sandwich-type immunocomplex. Moreover, the number of as-formed immunocomplex increased with increasing IL-37 concentration. It is worth noting that only weak redox peaks could be observed in the CV curves of AuNP-PDA and HRP-anti-IL-37-AuNP-PDA@graphene after the sole addition of OPD (2.0 mM) into PBS. Differently, when both OPD (2.0 mM) and H_2O_2 (4.0 mM) were added into PBS, a pair of redox

peaks in the CV curve of HRP-anti-IL-37-AuNP-PDA@graphene was clearly obtained. The anodic peak potential was -0.512V which can be ascribed to the redox of 2,2′-diaminoazobenzene, while the cathodic peak potentials was -0.593 V, which is related to enzymatic products. This suggests that the addition of H_2O_2 can accelerate the oxidation process of OPD under the catalysis of HRP, and the HRP shows high enzymatic catalytic activity for above oxidation process.
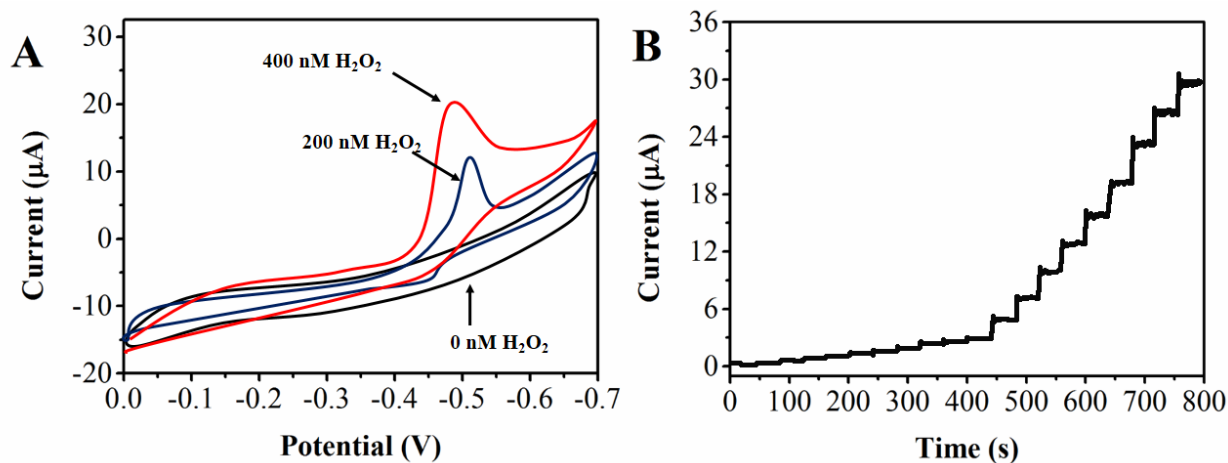
Figure 2. (A) Cyclic voltammograms of AuNP-PDA/ITO in PBS (pH=7) with 0, 200, and 400 nM H_2O_2, scan rate: 100 mV/s. (B) Catalytic electrochemical reduction of hydrogen peroxide over AuNP-PDA/ITO at −0.5 V with different H_2O_2 concentrations.

For comparison study, the amperometric responses to immunoreaction over HRP-anti-IL-37, AuNP-HRP-anti-IL-37, graphene-HRP-anti-IL-37 and HRP-anti-IL-37-AuNP-PDA@graphene were also performed using a secondary conjugating antibody, and the results were listed in Figure 3B. The loading of enzyme is defined as the total added enzyme minus by the residual enzyme after immobilization. As shown in Figure 3B, the samples using HRP and AuNP-PDA@graphene possess much larger amperometric change than that using others.
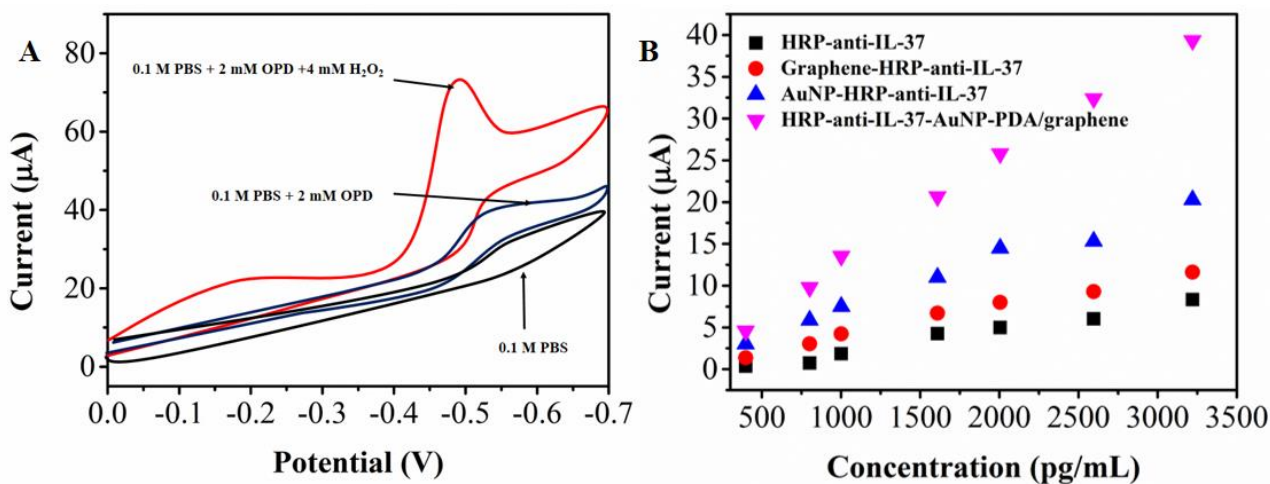
Figure 3. (A) Cyclic voltammograms of HRP-anti-IL-37-AuNP-PDA@graphene in 0.10 M PBS (pH=7) containing only OPD (2.0 mM) and both OPD (2.0 mM) and H_2O_2 (4.0 mM), respectively. (B) Amperometric responses of different immunosensors under various IL-37 concentrations.

The best performance of AuNP-PDA@graphene may be attributed to the following reasons. First of all, the density of immobilized HRP-anti-IL-37 might be greatly enhanced owing to the high surface to volume ratio of the bionanocomposite. Secondly, the capability of electron transfer was greatly improved (i.e., electrons could be effectively transferred from the electrode surface to the HRP redox center) by the doping of graphene and AuNP into the bionanocomposite. Additionally, adding PDA may enhance the attachment between graphene and AuNPh, and amplify output of amperometric signal.

To obtain the quantitative range and sensitivity of the proposed immunoassay, a sandwich immunoassay format was utilized for the determination of IL-37 over AuNP-PDA@graphene using labelled HRP-anti-IL-37 molecules as tracer, H_2O_2 as enzyme substrate and OPD as mediator. As shown in Figure 4, amperometric current of each sensor achieve steady state very rapidly after the addition of H_2O_2. Moreover, with an increase of IL-37 concentration from 4.0 to 800 pg/mL, amperometric current increased linearly. The detection limit of this sensor is 1.0 pg/mL ($S/N = 3$). This high sensitivity of the sensor can be attributed to the combination of a great number of HRP-anti-IL-37 molecules onto the AuNP-PDA@graphen. This can greatly enhance the interaction between antigen and antibody, especially under the condition of low antigen concentration in the sample. In addition, adding PDA showed positive effect on the adsorption of AuNP, and more Ab_1 molecules can be adsorbed. The amount of AuNP was also increased. Therefore, sensitivity of the immunosensor was improved. From Figure 4B, a linear regression $I(\mu A) = 1.322 + 0.08547c$ (pg/mL) can be obtained as well. Table 1 shows the comparison of our proposed IL-37 electrochemical sensor with some previously IL determination reports.
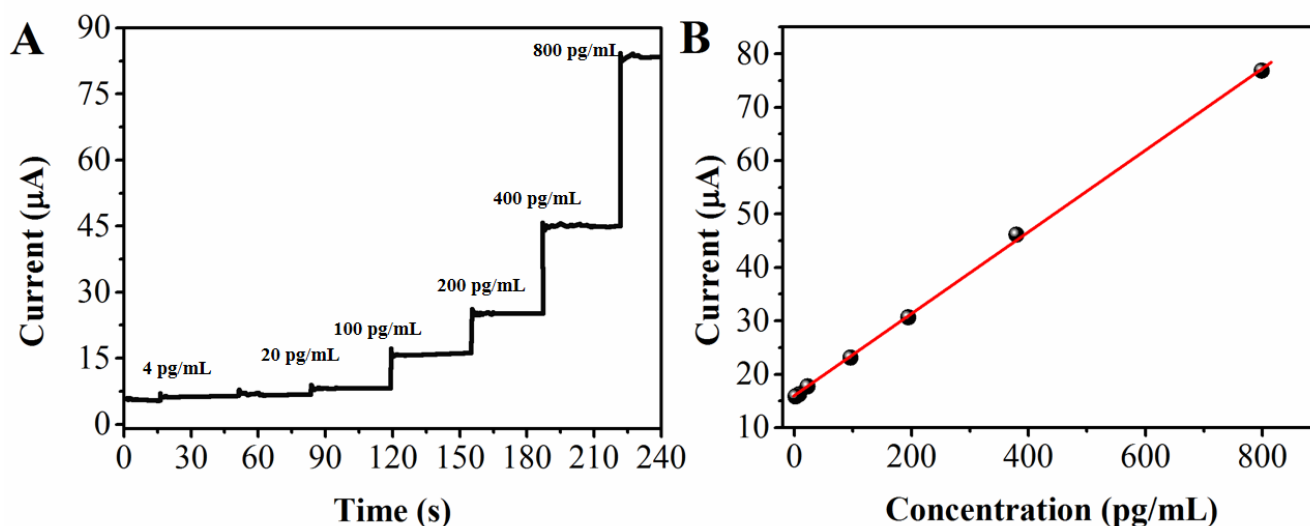
Figure 4. Amperometric results over immunosensors with different IL-37 concentrations: (A) steady-state amperometric current at −0.6 V in PBS (pH=7); (B) calibration plot IL-37 ($n = 3$) over immunosensor.

Table 1. Comparison of proposed IL-37 electrochemical sensor with other IL determination reports.

Method	Target molecules	LDR	LOD (µM)	Reference
Enzyme-linked immunosorbent assay	IL-10	5-100	2.4	[40]
Multidimensional heteronuclear magnetic resonance spectroscopy.	IL-4	8-129	2	[41]
Enzyme-linked immunosorbent assay	IL−1	—	—	[42]
Chemically synthesized analogs.	IL-8	20-100 pg/mL	4	[43]
Graphene-copper	IL-37	4.0 to 800 pg/mL	1 pg/mL	This work

Usually, performance of amperometric immunosensor greatly depends on the incubation temperature, time and pH value of working buffer. Therefore, the above-mentioned factors were investigated. The effect of pH value of working solution on the electrochemical behavior of immunosensor was firstly measured. As shown in Figure 5A, CV results of the immunosensor in PBS were obtained. PH values were adjusted from 3.0 to 9.0. With the increase of pH value, peak currents firstly increased at the lower pH range and then decreased at higher range, which might resulted from the decomposition of the antibody-antigen complex at low pH and by the inactivation of enzyme at high pH. In comparison with the CV response at high pH value, the result obtained at lower pH range was much better. This can be ascribed to that the protonation state of PDA can easily combine with the negatively charged AuNP. Therefore, pH value of working buffer was adjusted to 7 for the following experiments.

The dependences of immunocomplex formation on the incubation temperature and time were also studied, and the results were shown in Figure 5B. The responses gradually increased with increasing temperature and the maximum value was obtainedat 37 °C. Therefore, the incubation temperature was determined to be 37 °C. And then, the obtained immunosensor was incubated in a standard antigen solution at this temperature for different time. Similarly, the response increased gradually with incubation time and achieved a maximum value at 60 min (Figure 5C). Therefore, 60 min was defined as the incubation time and used in the following experiments.
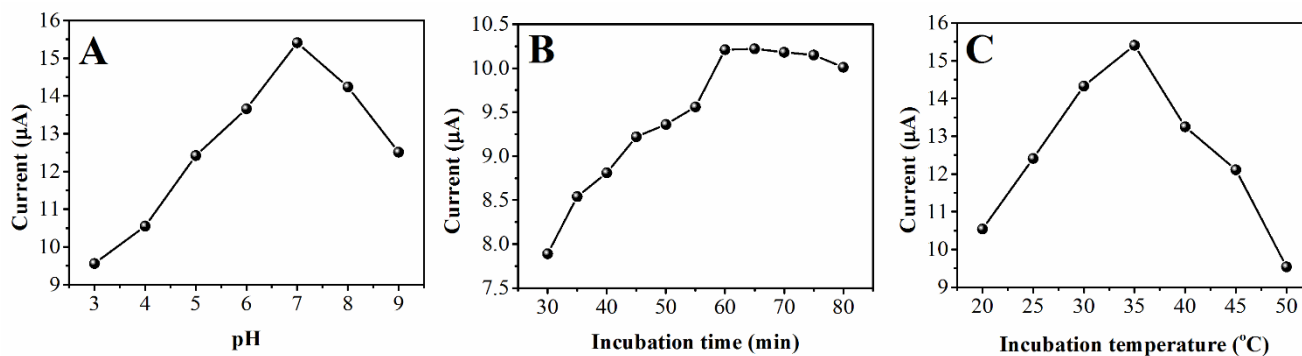
Figure 5. Influence of (A) pH value, (B) incubation temperature and (C) incubation time on immunosensor.

In order to evaluate the capability of the developed modified electrode in the detection of IL-37, the response behaviors of IL-37 with different real simples were examined. In addition, five clinical serum samples containing IL-37 were further examined using the proposed immunosensor. For comparison, conventional ELISA method was also employed, and the results were listed in Table 2. The relative errors of each method was calculated to be less than 4.45%. This reveals that the proposed immunosensor is available for clinical analysis, and it serves an important alternative for diabetes diagnosis.

Table 2. Determination of IL-37 in clinical serum samples.

Sample	Immunosensor (pg/mL)	ELISA (pg/mL)	RSD (%)
1	75.4	75.5	4.41
2	150.3	152.0	3.66
3	203.4	198.4	3.98
4	305.2	301.9	3.21
5	504.7	512.6	5.98

4. CONCLUSIONS

In conclusion, immunosensors based on AuNP-PDA and HRP-anti-IL-37-AuNP−PDA@graphene were prepared using a "sandwich-assay" method. As an efficient biointerface film with biocompatibility, AuNP-PDA can greatly enhance the conductivity, enlarge the specific surface area of the sensing interface, and thus contribute to the efficient immobilization of Ab_1. The proposed method can be utilized for the determination of IL-37 within the concentration from 4.0 to 800 pg/mL, and the detection limit is 0.8 pg/mL ($S/N = 3$). The presented strategy can be employed to improve sensitivity of immunoassay and prolong the lifetime. It is of great potential prospect for clinical immunoassay.

References

1. D. Accili, *Diabetes*, 53 (2004) 1633.
2. J.I. Odegaard and A. Chawla, *Science*, 339 (2013) 172.
3. A. Ceriello and E. Motz, *Arteriosclerosis, thrombosis, and vascular biology*, 24 (2004) 816.
4. M. Bensellam, D.R. Laybutt and J.-C. Jonas, *Molecular and cellular endocrinology*, 364 (2012) 1.
5. D.J. Freeman, J. Norrie, M.J. Caslake, A. Gaw, I. Ford, G.D. Lowe, D.S.J. O'Reilly, C.J. Packard and N. Sattar, *Diabetes*, 51 (2002) 1596.
6. S.M. Boekholdt and E.S. Stroes, *The Lancet*, 379 (2012) 1176.
7. V. Mohamed-Ali, S. Goodrick, A. Rawesh, D. Katz, J.M. Miles, J. Yudkin, S. Klein and S. Coppack, *The Journal of Clinical Endocrinology & Metabolism*, 82 (1997) 4196.

8. V. Mohamed-Ali, S. Goodrick, K. Bulmer, J.M. Holly, J.S. Yudkin and S.W. Coppack, *American Journal of Physiology-Endocrinology And Metabolism*, 277 (1999) E971.
9. A. Steensberg, G. Hall, T. Osada, M. Sacchetti, B. Saltin and B.K. Pedersen, *The Journal of physiology*, 529 (2000) 237.
10. M.A. Febbraio, P. Ott, H.B. Nielsen, A. Steensberg, C. Keller, P. Krustrup, N.H. Secher and B.K. Pedersen, *American Journal of Physiology-Endocrinology And Metabolism*, 285 (2003) E397.
11. J. Peake, P. Della Gatta, K. Suzuki and D. Nieman, *Exercise immunology review*, 21 (2015) 8.
12. A. Steensberg, C. Keller, R.L. Starkie, T. Osada, M.A. Febbraio and B.K. Pedersen, *American Journal of Physiology-Endocrinology and Metabolism*, 283 (2002) E1272.
13. R.J. Perry, J.-P.G. Camporez, R. Kursawe, P.M. Titchenell, D. Zhang, C.J. Perry, M.J. Jurczak, A. Abudukadier, M.S. Han and X.-M. Zhang, *Cell*, 160 (2015) 745.
14. S. Glund, A. Deshmukh, Y.C. Long, T. Moller, H.A. Koistinen, K. Caidahl, J.R. Zierath and A. Krook, *Diabetes*, 56 (2007) 1630.
15. A. Steensberg, C.P. Fischer, M. Sacchetti, C. Keller, T. Osada, P. Schjerling, G. Hall, M.A. Febbraio and B.K. Pedersen, *The Journal of physiology*, 548 (2003) 631.
16. K. Fosgerau, P. Galle, T. Hansen, A. Albrechtsen, C. de Lemos Rieper, B.K. Pedersen, L.K. Larsen, A.R. Thomsen, O. Pedersen and M.B. Hansen, *Journal of Endocrinology*, 204 (2010) 265.
17. P.A. Halban, K.S. Polonsky, D.W. Bowden, M.A. Hawkins, C. Ling, K.J. Mather, A.C. Powers, C.J. Rhodes, L. Sussel and G.C. Weir, *Diabetes Care*, 37 (2014) 1751.
18. C.K. Turner, T.M. Blieden, T.J. Smith, S.E. Feldon, D.C. Foster, P.J. Sime and R.P. Phipps, *Journal of immunological methods*, 291 (2004) 63.
19. H. Wu, Q. Huo, S. Varnum, J. Wang, G. Liu, Z. Nie, J. Liu and Y. Lin, *The Analyst*, 133 (2008) 1550.
20. K. Liang, W. Mu, M. Huang, Z. Yu and Q. Lai, *Electroanalysis*, 18 (2006) 1505.
21. L. Luo, Z. Zhang, L. Hou, J. Wang and W. Tian, *Talanta*, 72 (2007) 1293.
22. R. Kapoor and C.-W. Wang, *Biosensors and Bioelectronics*, 24 (2009) 2696.
23. R. Malhotra, V. Patel, J.P. Vaqué, J.S. Gutkind and J.F. Rusling, *Anal. Chem.*, 82 (2010) 3118.
24. C. Deng, F. Qu, H. Sun and M. Yang, *Sensors and Actuators B: Chemical*, 160 (2011) 471.
25. N.P. Sardesai, J.C. Barron and J.F. Rusling, *Anal. Chem.*, 83 (2011) 6698.
26. Y. Li, M. Liu, C. Xiang, Q. Xie and S. Yao, *Thin Solid Films*, 497 (2006) 270.
27. S.H. Ku, J.S. Lee and C.B. Park, *Langmuir*, 26 (2010) 15104.
28. H. Lee, S.M. Dellatore, W.M. Miller and P.B. Messersmith, *science*, 318 (2007) 426.
29. Y. Fu, P. Li, L. Bu, T. Wang, Q. Xie, X. Xu, L. Lei, C. Zou and S. Yao, *J Phys Chem C*, 114 (2010) 1472.
30. Y. Fu, P. Li, T. Wang, L. Bu, Q. Xie, X. Xu, L. Lei, C. Zou, J. Chen and S. Yao, *Biosensors and Bioelectronics*, 25 (2010) 1699.
31. S. Peng, G. Zou and X. Zhang, *Journal of Electroanalytical Chemistry*, 686 (2012) 25.
32. L. Zhao, S. Li, J. He, G. Tian, Q. Wei and H. Li, *Biosensors and Bioelectronics*, 49 (2013) 222.
33. T. Li, M. Yang and H. Li, *Journal of electroanalytical chemistry*, 655 (2011) 50.
34. L. Zheng, L. Xiong, Y. Li, J. Xu, X. Kang, Z. Zou, S. Yang and J. Xia, *Sensors and Actuators B: Chemical*, 177 (2013) 344.
35. E. Asadian, S. Shahrokhian, A. Iraji Zad and F. Ghorbani-Bidkorbeh, *Sensors and Actuators B: Chemical*, 239 (2017) 617.
36. P. Lv, X.-W. Tan, K.-H. Yu, R.-L. Zheng, J.-J. Zheng and W. Wei, *Carbon*, 99 (2016) 222.
37. J. Zhao, Y. Liu, X. Quan, S. Chen, H. Zhao and H. Yu, *Electrochimica Acta*, 204 (2016) 169.
38. R.M. Torrenterodríguez, S. Campuzano, M.V. Ruizvaldepeñas, M. Gamella and J.M. Pingarrón, *Biosensors & bioelectronics*, 77 (2016) 543.
39. I.D. Dano, O.O.M. Oukem-Boyer, A.E. Mahamane and H. Sadou, *Journal of Biological Sciences*, 16 (2016) 136.
40. M.W.V.D. Linden, T.W.J. Huizinga, D.J. Stoeken, A. Sturk and R.G.J. Westendorp, *Journal of*

    Immunological Methods, 218 (1998) 63.
41. R. Powers, D.S. Garrett, C.J. March, E.A. Frieden, A.M. Gronenborn and G.M. Clore,
    Biochemistry, 32 (1993) 6744.
42. N. Demircan, B.G. Safran, M. Soylu, A.A. Ozcan and S. Sizmaz, *Eye*, 20 (2006) 1366.
43. I. Clark-Lewis, C. Schumacher, M. Baggiolini and B. Moser, *Journal of Biological Chemistry*, 266
    (1991) 23128.